



Observations of Correlated Broadband Electrostatic Noise and Electron Cyclotron Emissions in the Plasma Sheet

Prepared by

J. L. ROEDER
Space and Environment Technology Center
Technology Operations
The Aerospace Corporation

V. ANGELOPOULOS
Department of Physics
University of California, Los Angeles, CA

W. BAUMJOHANN
Max-Planck Institute for Physics and Astrophysics
Institute for Extraterrestrial Physics

R. R. ANDERSON
Department of Physics and Astronomy
University of Iowa

15 November 1991

Prepared for

SPACE SYSTEMS DIVISION
AIR FORCE SYSTEMS COMMAND
Los Angeles Air Force Base
P.O. Box 92960
Los Angeles, CA 90009-2960

403965

92-23659



80/89

Engineering and Technology Group

DTIC
ELECTE
AUG 26 1992
S A D

✓ *Original contains color plates: All DTIC reproductions will be in black and white*

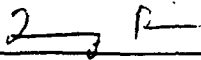
THE AEROSPACE CORPORATION
El Segundo, California

APPROVED FOR PUBLIC RELEASE;
DISTRIBUTION UNLIMITED

This report was submitted by The Aerospace Corporation, El Segundo, CA 90245-4691, under Contract No. F04701-88-C-0089 with the Space Systems Division. P. O. Box 92960, Los Angeles, CA 90009-2960. It was reviewed and approved for The Aerospace Corporation by A. B. Christensen, Principal Director, Space and Environment Technology Center. Robert D. Mullaney was the project officer for the Mission-Oriented Investigation and Experimentation (MOIE) program.

This report has been reviewed by the Public Affairs Office (PAS) and is releasable to the National Technical Information Service (NTIS). At NTIS, it will be available to the general public, including foreign nationals.

This technical report has been reviewed and is approved for publication. Publication of this report does not constitute Air Force approval of the report's findings or conclusions. It is published only for the exchange and stimulation of ideas.



QUANG BUI, Lt, USAF
MOIE Program Manager



ROBERT D. MULLANY, Capt, USAF
Chief, FEWS Sensors Division

PREFACE

The authors are indebted to G. Paschmann and H. Luhr for helpful discussions and for the use of the IRM plasma and magnetometer data. The work performed at The Aerospace Corporation was supported by the US Air Force System Command's Space System Division under Contract No. F04701-88-C-0089. Computing resources were provided by the Pittsburg Supercomputing Center.

| | |
|---------------|----------------------|
| Accession For | |
| NTIS CRA&I | ✓ |
| DTIC TAB | |
| Unannounced | |
| Justification | |
| By | |
| Distribution/ | |
| Availability | |
| Dist | Avail and/or Spec |
| A-1 | |

DTIC QUALITY INSPECTION

CONTENTS

| | |
|---------------------|----|
| INTRODUCTION..... | 5 |
| OBSERVATIONS..... | 7 |
| LINEAR THEORY | 11 |
| CONCLUSIONS..... | 15 |
| REFERENCES..... | 17 |

FIGURES

| | |
|---|----|
| 1. Spectrogram of the electric field spectral density..... | 8 |
| 2. Electric field spectrum averaged over 60 s during the broadband and cyclotron emissions | 9 |
| 3. Temporal growth rate envelopes of all growing modes at all wave numbers and angles of propagation for several beam velocities..... | 12 |
| 4. Marginal stability curves for the lowest frequency cold electron cyclotron mode as a function of the model parameters of the hot electron loss cone distribution..... | 13 |

INTRODUCTION

The electrostatic plasma wave emissions detected in the Earth's magnetotail include broadband electrostatic noise and electron cyclotron emissions. These two types of waves were observed previously to be uncorrelated with one another, and they were assumed to be generated by two separate and unrelated processes. In this paper, we report several observations by the AMPTE Ion Release Module (IRM) of broadband electrostatic noise and cyclotron emissions that exhibit a high degree of correlation in time. An explanation of the generation of both emissions is presented that involves an indirect link between two plasma instabilities.

Broadband electrostatic noise (BEN) emissions are impulsive electric field variations over a very wide range of frequency [Gurnett *et al.*, 1976]. Within the plasma sheet boundary layer, BEN emissions have been observed to correlate with the occurrence of ion beams, and many theories attempt to explain the wave generation by various ion beam instabilities [Schriver and Ashour-Abdalla, 1987]. On the other hand, there are also intervals in which BEN emissions have been observed without ion beams [Parks *et al.*, 1984]. Schriver and Ashour-Abdalla [1989] suggested that the waves during these periods were generated by field-aligned currents carried by cold electron beams.

Narrowband electric field emissions in the harmonic bands above the local electron cyclotron frequency have also been observed in the magnetosphere. These " $n+1/2$," or electron cyclotron harmonic (ECH) emissions, have been detected in the near-earth plasma sheet [Roeder and Koons, 1989] and in the more distant tail regions [Gurnett *et al.*, 1976]. These emissions have been attributed to instabilities involving a positive perpendicular gradient in the hot electron velocity distribution, such as a loss cone [Ashour-Abdalla and Kennel, 1978].

OBSERVATIONS

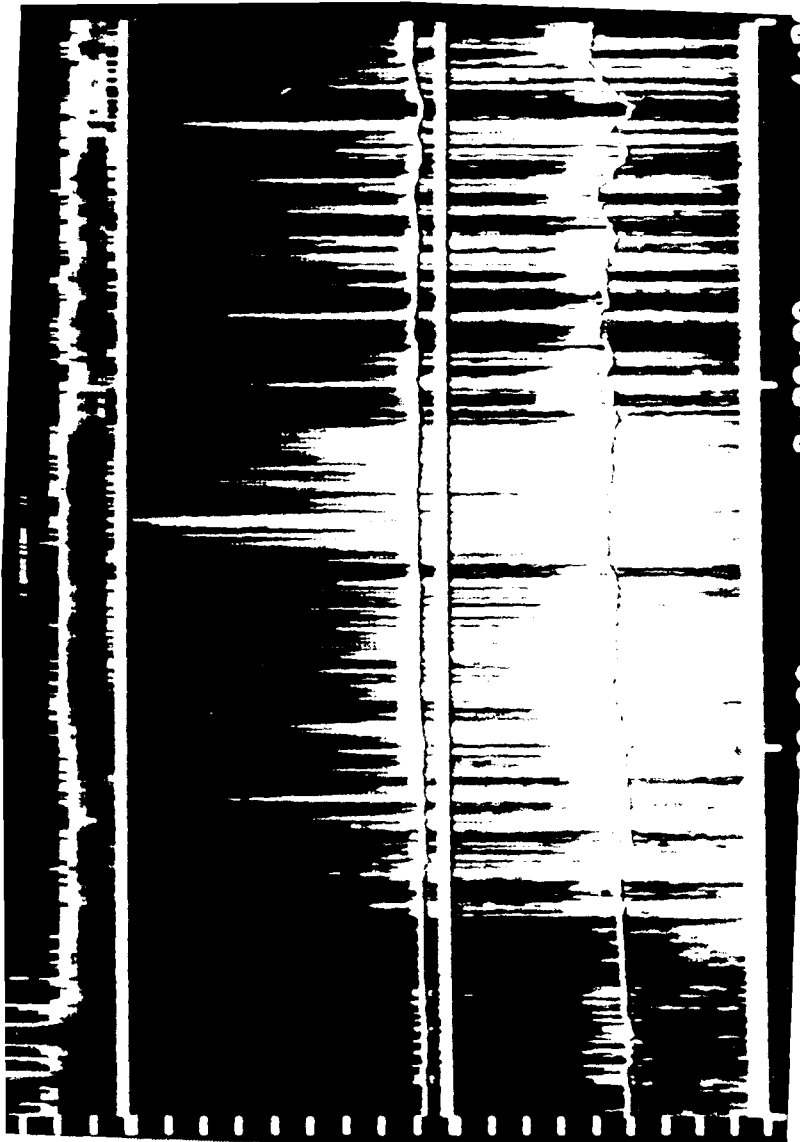
Four months of IRM data were examined using 1-hr spectrograms to find cases of correlated BEN and ECH waves. Four intervals were found in which such emissions were observed for more than five minutes. All of the cases occurred in the recovery phase of substorms when the spacecraft was in the central plasma sheet. One example, which occurred during a moderate substorm on 12 April 1986, has been analyzed in detail. The IRM was in the postmidnight sector at a radial distance of 11 to 14 R_e .

The electric field emissions observed on April 12, 1986, are shown in Figure 1 as a spectrogram of 12-s averages from the Aerospace Stepped Frequency Receiver (SFR). The figure is partitioned into three panels with the linear frequency scales of 0.2 to 2.6 kHz, 0.9 to 9.0 kHz, and 9 to 99 kHz, respectively. The frequency ranges of the middle and bottom panels overlap so that many features are displayed twice in the spectrogram. The lines in the lower panels mark the local electron cyclotron frequency, f_{ce} .

An analysis of the plasma and magnetic field data showed that the spacecraft was in the magnetotail lobe at the beginning of the contact. Several encounters with the plasma sheet boundary layer were noted in the interval 0200-0210 UT. Near 0210 UT, the IRM entered the central plasma sheet and remained in that region until the end of the pass at 0500 UT. Bursts of impulsive, broadband emissions were detected in the frequency range 0.2 to 10 kHz when the plasma sheet boundary layer was encountered in the interval 0200-0210 UT. After entering the central plasma sheet at 0215 UT, the receiver continued to observe intense broadband emissions continuously until 0325 UT and sporadically thereafter. Enhancements of the electric field spectrum were also observed at frequencies near 1.2 to 1.3 f_{ce} . The occurrence of these peaks near f_{ce} was correlated with the simultaneous occurrence of the impulsive broadband emissions.

Figure 2 presents the electric field spectrum from the swept-frequency receiver (SFR) and the University of Iowa 16-channel ELF/MF instrument during one of the most intense bursts of waves. The BEN emission was measured to be a broad enhancement from approximately 30 Hz to 10 kHz. The enhancement just above f_{ce} is clearly visible in this spectrum. If this peak is deleted from the spectrum, the remaining broadband emission has a total integrated amplitude of 0.1 mV/m. The ECH feature itself has an amplitude of 0.15 mV/m, a center frequency of 1.25 f_{ce} , and a relative bandwidth of 18%, consistent with previously observed ECH wave emissions [Roeder and Koons, 1989].

A polarization analysis was also performed on the electric field data by sorting the data into bins according to the angle between the dipole antenna and the measured magnetic field. The angular coverage by the antenna (15° to 90°) was sufficient to show that the broadband impulsive emissions were aligned parallel to the magnetic field, and that the cyclotron emissions were polarized perpendicular to the magnetic field. This result lends credence to the interpretation that the narrow-band enhancement above f_{ce} was a cyclotron wave mode and not just enhanced growth of the broadband emissions in a limited frequency range. The time series of the 10-s average amplitudes of both emissions were computed by integrating suitably edited spectra. An analysis of these series revealed a peak in the cross correlation function of 0.43 at a time lag of 20 to 30 s with the BEN emission occurring first. Several intervals in the data appeared to have a one-to-one correspondence between bursts of the two emissions, but the intensities of the bursts seemed unrelated.



The particle distributions observed during the BEN and ECH emissions were typical of the central plasma sheet [Baumjohann *et al.*, 1989]. No ion beams were observed in the energy range of the instrument (0.02 to 40 keV). The higher energy electron and ion measurements are well represented by nearly isotropic Maxwellian distributions with densities and temperatures of $n_h \approx 0.3 \text{ cm}^{-3}$, $T_h \approx 400\text{--}500 \text{ eV}$, and $n_i \approx n_h$, $T_i \approx 3.5\text{--}4.3 \text{ keV}$, respectively. In the range 0.020 to 0.060 keV, the electron distribution is uncertain because the data is contaminated by photoelectrons; however, we believe that a pronounced field-aligned anisotropy at these energies provides circumstantial evidence of cold electron beams streaming upward, presumably from the ionosphere. These cold beam electrons are best fitted to a Maxwellian distribution of density $n_c \approx 0.01 \text{ cm}^{-3}$, $T_h \approx 1 \text{ eV}$, and a field-aligned bulk velocity $U_c \approx 1000 \text{ km/s}$. Due to the uncertainty of the photoelectrons and the coarse energy resolution of the measurement, these values are upper limits on the beam population. The higher-energy electron data showed a small temperature anisotropy, but the angular resolution of the plasma instrument is too coarse to observe the loss cone.

The observations show that the AMPTE IRM detected time correlated BEN and ECH wave emissions in the central plasma sheet for over an hour. The BEN emissions were polarized predominantly parallel to the static magnetic field, and the ECH emissions exhibited near perpendicular polarization. No ion beams were observed, but electron beams were detected streaming upward along the magnetic field at low energies.

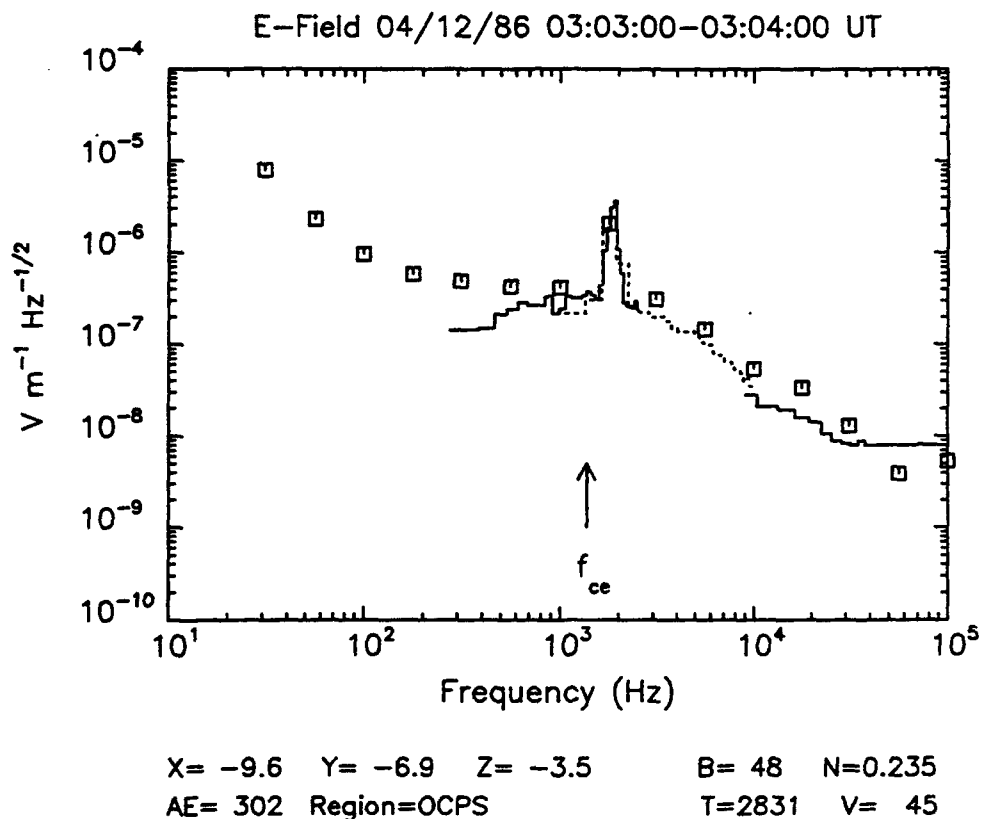


Figure 2. Electric field spectrum averaged over 60 s during the broadband and cyclotron emissions.

LINEAR THEORY

To explain the generation of the waves, the observed plasma was modeled by a three-component Maxwellian distribution, in which a cold electron beam drifts along the magnetic field with a velocity U_c relative to a stationary, hot background plasma. The density, n_s , and temperature, T_s , (thermal speed u_s) of each component were chosen to be consistent with the plasma data, where the subscript $s = c, h, i$ denote the cold beam electrons, the hot background electrons, and the background ions, respectively. The parameters are restricted by: $T_i \cong T_h$, $T_c \ll T_h$, $n_c < n_h$, with the total density $n_t = n_i = n_h + n_c$, and $U_c \leq u_h$. The analysis assumes that the wave frequency is above $(\Omega_{ce}\Omega_{pi})^{1/2}$.

The two-component electron distribution makes the electron acoustic instability a natural candidate for the wave generation. If the cold electron component is a beam drifting relative to the hot component, the slow electron acoustic mode may grow due to a resonance with the negative slope of the ions and/or the hot electrons at the expense of the beam kinetic energy. To investigate the generation of the ECH waves by this process, we include a magnetic field ($\Omega_{ce} < \Omega_{pe}$). Its presence is found to distort the dispersion and reduce the growth rate of the oblique electron acoustic modes.

Figure 3 summarizes a numerical study of the magnetized electrostatic plasma dispersion relation. The values of the plasma parameters are $n_c/n_{tot} = 0.05$, $T_c/T_h = 2 \times 10^{-3}$, and $\Omega_{ce}/\Omega_{pe} = 0.25$. The envelopes of the maximum growth rate are shown for all growing modes at all wavenumber vectors (irrespective of the branch where the growth occurs). Each curve is labeled with its value of the beam drift speed. The high-frequency peaks correspond to the electron acoustic instability driven by the hot electrons and the low-frequency peaks correspond to the ion-driven instability. The dashed curve corresponds to the same parameters as the solid curve of $U_c = 1.25 u_h$, but it is run for $\Omega_{ce} = 0$ and is shown for comparison with the magnetized case. At the observed beam velocity of $0.1 u_h$, the high-frequency hot electron-driven instability is stabilized, and the growth of the ion/ion instability is nonzero only near $0.02 \Omega_{pe}$. This is a significant discrepancy between the theory and the observed wave spectrum, implying the need for a more elaborate model.

The smooth growth rates of the electron acoustic instability could possibly explain the BEN waves, but cannot account for the ECH emissions. If we assume that the electron beam was the free energy source of the BEN waves, then it must have some significance in the generation of the ECH emissions since the two types of waves exhibit a high degree of correlation. ECH wave generation by an electron beam has been observed in laboratory plasmas [Seidl, 1970], but this mechanism cannot reproduce our observations because the ECH modes of the hot electrons are severely damped at large wavenumbers (i.e., for $k_{\perp} > \rho_h^{-1}$), unless one assumes almost perpendicular propagation, which gives a lower limit for the beam velocity required to excite the first harmonic mode - $(U_c)_{min} > \omega/k \approx \Omega_{ce}/k_{\parallel} \gg u_h$ - which is large compared to our observations. This is corroborated by Figure 3, where for a beam velocity as high as $1.25 u_h$ there is no peak near the cyclotron frequency. In addition, electron beams usually generate higher harmonic emissions, yet our measurements show no second harmonic emissions.

To explain the ECH waves, one must assume a perpendicular gradient in the electron velocity distribution for a free energy source. Most theories of ECH emissions use a loss cone in the hot electron distribution. Young [1973] showed that a mild loss cone feature embedded in an electron distribution

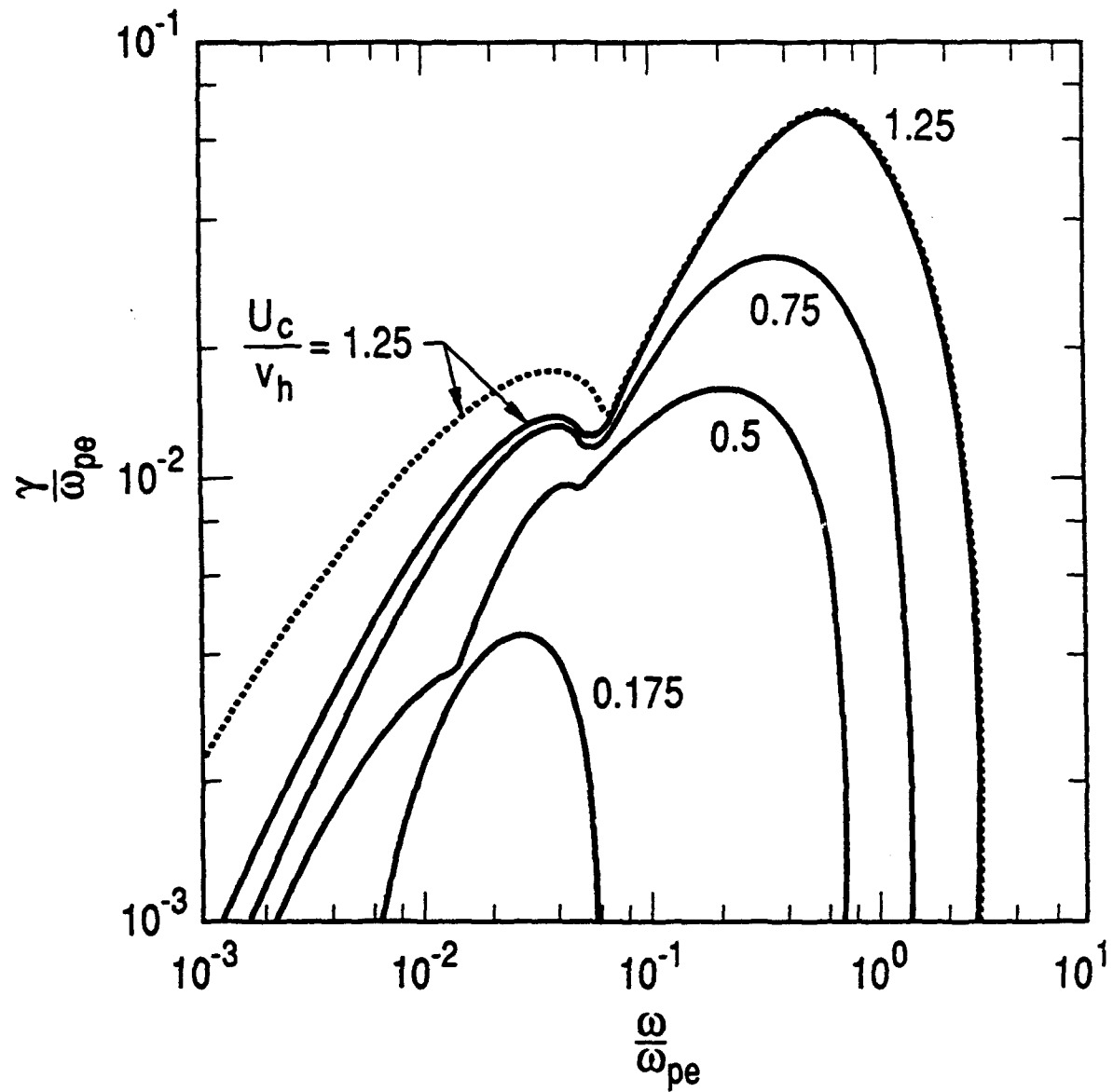


Figure 3. Temporal growth rate envelopes of all growing modes at all wave numbers and angles of propagation for several beam velocities.

cannot give growth to ECH waves unless another much colder electron component is present. The presence of the cold electrons is essential to modify the wave phase velocities in order to achieve resonance with the free energy source in the hot electrons. The Doppler shift of the perpendicular ECH modes is small, so that any streaming of the cold electrons becomes irrelevant. This provides an indirect link between the two instabilities: the beam electrons generate the BEN and also provide the ECH modes that grow due to an already existing loss cone structure of the hot electrons.

The angular resolution of the IRM plasma instrument is too coarse to observe a realistic loss cone. To make plausible the generation of the ECH waves, we have determined that such a small, unobservable feature could provide enough free energy for the instability. We solved the electrostatic dispersion relation for the model plasma, relaxing the beam velocity to zero and imposing a loss cone on the hot electron velocity distribution function. The loss cone is provided by a subtracted Maxwellian distribution [Ashour-Abdalla and Kennel, 1978, equation (5)], which is characterized by a "filling" parameter Δ and a "sharpness" parameter β . Figure 4 shows the results as the marginally stable Δ versus frequency for a given β . As β becomes larger, more particles have to be subtracted from the loss cone (decreasing Δ) for the unstable spectrum to remain unstable at frequencies of 1.2 to 1.3 Ω_{ce} . This shows that a sharp, but almost filled-in, loss cone may be responsible for the observed ECH waves.

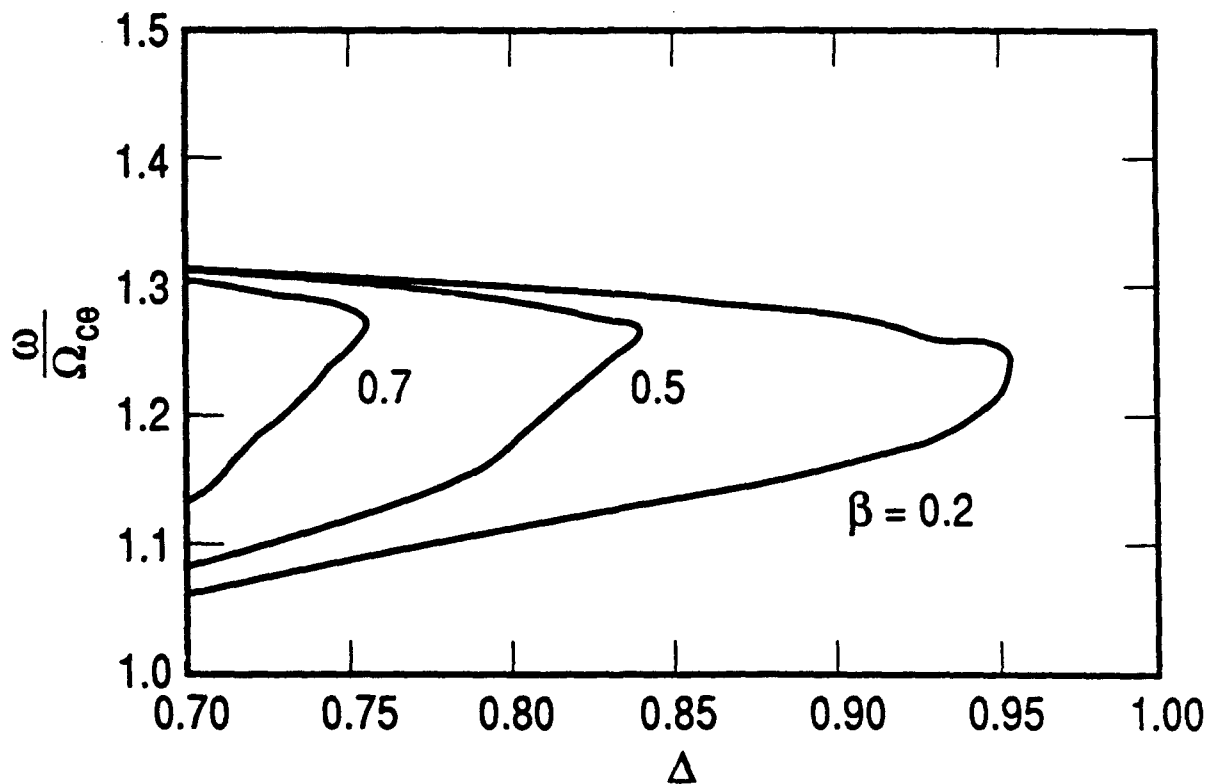


Figure 4. Marginal stability curves for the lowest frequency cold electron cyclotron mode as a function of the model parameters of the hot electron loss cone distribution.

CONCLUSIONS

In a four-month period the AMPTE IRM observed the correlated occurrence of BEN emissions and ECH emissions in four intervals in the central plasma sheet. The measured electric field spectrum consists of a broad feature in the range 30 Hz to 10 kHz and a narrowband enhancement at $1.2 f_{ce}$ (2.3 kHz). These two emissions tend to occur in bursts, with the ECH emission being detected on the trailing edge of the BEN burst. The plasma data exhibits hot particle distributions that are typical of the central plasma sheet, together with evidence of a low energy electron beam streaming upward through the hot plasma. Linear plasma theory indicates that the BEN emissions may have been generated by the beam electrons via the electron acoustic instability, although the growth of this instability is restricted to a somewhat lower frequency range than the observed wave emissions. The calculation also indicates that this process could not be the source of the ECH waves. It is proposed that the ECH emissions were generated by a loss cone instability driven by an anisotropy in the hot electron distribution, which was too small to be observed by the plasma instrument. The correlation of the two emissions is due to the destabilizing action of the cold electrons on both of the instabilities.

REFERENCES

- Ashour-Abdalla, M., and C. F. Kennel, Nonconvective and convective electron cyclotron harmonic instabilities, *J. Geophys. Res.*, **83**, 1531, 1978.
- Baumjohann, W., G. Paschmann, and C. A. Cattell, Average plasma properties in the central plasma sheet, *J. Geophys. Res.*, **94**, 6597, 1989.
- Gurnett, D. A., L. A. Frank, and R. P. Lepping, Plasma waves in the magnetotail, *J. Geophys. Res.*, **81**, 6059, 1976.
- Parks, G. K., M. McCarthy, R. J. Fitzenreiter, J. Etcheto, K. A. Anderson, R. R. Anderson, T. E. Eastman, L. A. Frank, D. A. Gurnett, C. Huang, R. P. Lin, A. T. Y. Lui, K. W. Ogilvie, A. Pedersen, H. Reme, and D. J. Williams, Particle and field characteristics, of the high-latitude plasma sheet boundary layer, *J. Geophys. Res.*, **89**, 8885, 1984.
- Roeder, J. L., and H. C. Koons, A survey of electron cyclotron waves in the magnetosphere and the diffuse auroral electron precipitation, *J. Geophys. Res.*, **94**, 2529, 1989.
- Schrifer, D., and M. Ashour-Abdalla, Generation of high-frequency broadband electrostatic noise: the role of cold electrons, *J. Geophys. Res.*, **92**, 5807, 1987.
- Schrifer, D., and M. Ashour-Abdalla, Broadband electrostatic noise due to field-aligned currents, *Geophys. Res. Lett.*, **16**, 899, 1989.
- Seidl, M., Temperature effects on high-frequency beam plasma interaction, *Phys. Fluids*, **13**, 966, 1970.
- Young, T. S. T., J. D. Callen, and J. E. McCune, High-frequency electrostatic waves in the magnetosphere, *J. Geophys. Res.*, **78**, 1082, 1973.